Energy Partitioning During an Earthquake

Hiroo Kanamori

Seismological Laboratory, California Institute of Technology, Pasadena, California, USA

Luis Rivera

EOST-IPGS; Université Louis Pasteur, Strasbourg, France

We investigate the partitioning of energy released during an earthquake to radiated, fracture and thermal energies in an attempt to link various observational results obtained in different disciplines. The fracture energy, E_G, used in seismology is different from that commonly used in mechanics where it is the energy used to produce new crack surface. In the seismological language it includes the energies used for off-fault cracking, and various thermal processes. The seismic moment, M_0, the radiated energy, E_R, and rupture speed, V_R, are key macroscopic parameters. The static stress drop can be a complex function of space, but if an average can be defined as $\Delta\tau$, it is also a useful source parameter. From the combination of M_0, E_R, and, $\Delta\tau$ we can estimate the radiation efficiency η_R, or E_G which can also be estimated independently from V_R. η_R provides a link to the results of dynamic modeling of earthquakes which determines the displacement and stress on the fault plane. Theoretical and laboratory results can also be compared with earthquake data through η_R. Also, the fracture energy estimated from the measurement of the volume and grain size of gouge of an exhumed fault can be linked to seismic data through η_R. In these comparisons, the thermal energy is not included, and it must be estimated independently from estimates of sliding friction during faulting. One of the most challenging issues in this practice is how to average the presumably highly variable slip, stress and frictional parameters to seismologically determinable parameters.

INTRODUCTION

During an earthquake, the potential energy (mainly elastic strain energy and gravitational energy) stored in Earth is released as radiated energy, fracture energy, and thermal energy. Understanding the partitioning of energy is a key toward understanding the physics of earthquakes. As a useful analog of this process, we often consider the fracture of a solid. Rupture propagation in a solid material is an irreversible process. Some amount of energy must be continuously supplied near the rupture front to sustain its propagation. In the ideally brittle Griffith [1920] model of crack propagation, this energy is associated with creation of fresh new fault surfaces. Barenblatt [1959] completed this view by introducing a small "cohesive zone" behind the ideal rupture front, in which some work should be done to vanquish the cohesive stresses. However, during an earthquake, many additional physical processes take place near the rupture front and in the surrounding volume and contribute to the energy budget [e.g., Shipton et al., 2006a].

Earthquakes: Radiated Energy and the Physics of Faulting
Geophysical Monograph Series 170

10.1029/170GM03

Geological observations of pseudotachylytes along some exhumed faults are evidence for occasional melting within a region of a few mm to cm near the fault [Sibson, 1975]. If fluid exists in a fault zone, it will be pressurized upon heating. The thermal energy and latent heat associated with these processes should be considered in the energy balance [Terada 1930; Jeffreys, 1942; Sibson, 1973]. Some energy is also expended for near and off-fault cracking associated with fault rupture [Rice et al. 2005; Andrews 2005]. As a result of these processes, fault gouge is formed from which one can estimate the total energy expended during the life time of a fault [McGarr et al., 1979; Wilson et al., 2005, Chester et al., 2005]. We investigate the energy budget involved in these microscopic and macroscopic processes with the hope of linking the observational results obtained in structural geology, rock mechanics and seismology.

BASIC RELATIONS

The energy partitioning associated with faulting in a pre-stressed medium can be written in a concise form using the expressions derived by Kostrov [1974] and Dahlen [1977]. The radiated energy, E_R, in a homogeneous whole space can be written as

$$E_R = \frac{1}{2}\int_{\Sigma}\left(\sigma_{ij}^1 + \sigma_{ij}^2\right)\Delta u_i \nu_j dS - \int_{\Sigma} 2\gamma_{eff} dS - \int_{\Sigma} dS \int_{t_r(x)}^{t_2} \sigma_{ij}\Delta\dot{u}_i \nu_j dt \quad (1)$$

where dS is the surface element, Σ is an open surface representing the fault plane, and σ_{ij}, Δu_i, ν_j, $t_r(x)$, and t_2 are the stress, dislocation on Σ, a unit normal to Σ, the time when slip begins at point x on Σ, and an arbitrary time after the slip motion has ceased, respectively. The superscripts 1 and 2 refer to before and after the slip occurred. Rudnicki and Freund [1981] showed that this energy is equivalent to the radiated energy determined from the energy flux carried by P and S waves at far-field. Traditionally, this is the quantity seismologists measure as E_R after all the complex propagation effects arising from the finiteness and the three-dimensional structure of the Earth have been corrected for. More details on the definition of E_R are given in Rivera and Kanamori [2005].

The first term on the right-hand side is the change in the total potential energy (mostly elastic strain energy and the gravitational energy), the second term is the energy used to create the new surfaces on the edge of the expanding fault. Here, γ_{eff} is the surface energy. The third term is the work done on the fault plane during faulting. If we literally interpret the second term as the fracture energy near the crack tip only (in the sense of the Griffith [1920] theory), then this term can be ignored for most earthquakes, if the surface energy γ_{eff} of the order of 1 J/m^2, typical values for minerals and rocks, is used. In this case, as the fault plane increases in size, this term becomes relatively unimportant.

We will later discuss the relationship between this theoretical model and real faults.

SIMPLE MODEL

To facilitate interpretation of (1), we consider a simple shear fault for which σ_{ij}, σ_{ij}^1, σ_{ij}^2, and Δu_i are uniform on the fault with area A and given by scalars τ, τ_1, τ_2, and D, respectively [Rivera and Kanamori, 2005]. Then, neglecting the second term for the time being, (1) can be written as

$$E_R = \frac{1}{2}\left(\tau_1 + \tau_2\right)DA - A\int_0^D \tau dD \quad (2)$$

Figure 1 graphically shows these energies for a fault with unit area. In the text, we refer to energies for faults with area A by multiplying by A the energies shown in the figure. The potential energy change,

$$E_T = \frac{1}{2}\left(\tau_1 + \tau_2\right)DA$$

is given by the trapezoidal area AODC. The third term is the dissipated energy or the work done on fault plane; equation (2) means that it is the total energy minus the radiated energy. The stress on the fault plane can change in a complex

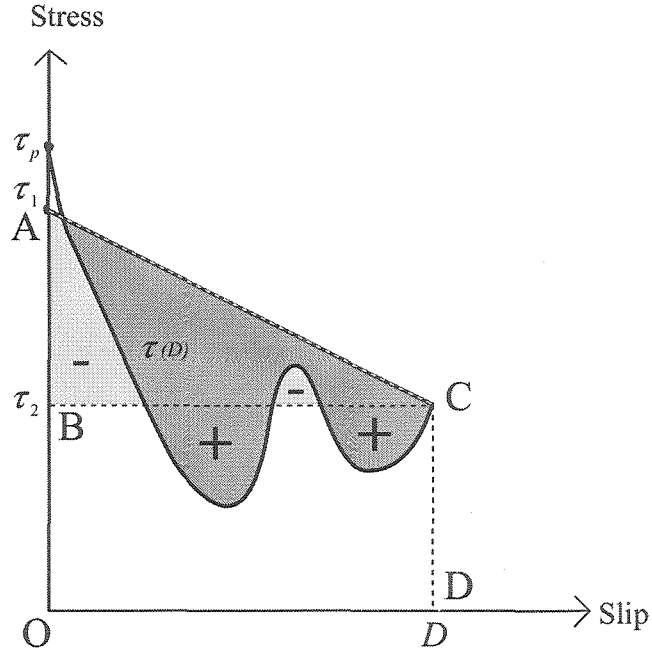

Figure 1. Graphic representation of the energy budget for a fault with unit area.

way depending on how it is released on the fault plane. Here, we assume that it initially increases from the initial stress τ_1 to τ_p to initiate slip. In this sense, the peak stress τ_p can be interpreted as the yield stress. Then, once slip motion begins, it drops rapidly, varies as given by the curve $\tau(D)$, and eventually drops to τ_2 when the slip stops. We note here that, in Figure 1, the line segments AC and CD just geometrically define E_T, but the curve $\tau(D)$ actually shows the trajectory of the stress change on the fault plane. The total energy dissipated is given by the area under $\tau(D)$ and corresponds to the second term of the right-hand side of equation 2. If we assume that the stress drops from τ_p to τ_1 very rapidly (e.g., for a brittle failure), we can ignore the difference between τ_1 and τ_p for purposes of energy estimation, and the radiated energy E_R which is the difference between E_T and the dissipated energy is given by the dark area. If the stress drops quasi-statically along AC, no energy is radiated (i.e., silent earthquake).

Equation (2) can also be written as

$$E_R = \frac{1}{2}(\tau_1 - \tau_2)DA - \left[A\int_0^D \tau dD - \tau_2 DA\right] \qquad (3)$$

The first term on the right-hand side,

$$E_{T0} = \frac{1}{2}(\tau_1 + \tau_2)DA,$$

is given by the triangular area ABC, and $\Delta\tau \equiv \tau_1 - \tau_2$ is the static stress drop. The term in the bracket on the right-hand side gives the difference between the areas labeled by + and –, which Kostrov [1974] called the "radiation friction". In some simplified seismological practice, the triangular area, E_{T0}, is taken as the radiated energy. Thus, in such a practice, as Kostrov [1974] pointed out, the term corresponding to the radiation friction is ignored in the estimation of E_R. However, in many other modern practices, E_R is measured either directly from the far-field displacements [e.g., Haskell, 1964; Boatwright and Choy, 1986] or indirectly by integration of (1) on the fault plane [Ide, 2002; Favreau and Archuleta, 2003]. Thus, in principle, the term corresponding to the radiation friction is correctly included in estimation of E_R, but, in practice, it is always difficult to accurately include the contributions from high-frequency seismic waves, because high-frequency energies are strongly attenuated and scattered during propagation. In seismological practice, the energy spectrum is often assumed to fall off as ω^{-2} (ω is the angular frequency) at high frequency beyond a corner frequency, and the integration is truncated at a cut-off frequency, which is several times the corner frequency. Recent dynamic fracture modeling (Madariaga et al., 2006) suggests that complex fault models with stress heterogeneities and geometrical kinks excite high-frequency seismic waves with an ω^{-2} spectral fall-off. In this case, however, extra energy is used near the tip of the kink, and the total radiated energy will decrease. When estimating the radiated energy from the spectra, we can account for this effect by properly choosing the cut-off frequency.

SLIP-WEAKENING MODEL

In general, in the case of an expanding crack, the stress increases from τ_1 to the yield stress τ_P at the beginning of the rupture process as illustrated in Figure 1, and then drops. (Hereafter, the terms crack and fault will be used interchangeably when a fault is approximated by a planar surface.) The curve given by $\tau(D)$ in Figure 1 schematically illustrates this, but the actual variation may be even more complex. Seismologically, it is difficult to determine the variation in detail. Only under certain circumstances, it has been determined from the slip distribution on the fault plane as a function of space and time [Ide and Takeo, 1997; Mikumo et al., 2003]. However, because of the technical difficulties in dealing with high-frequency waves, the result should be regarded as a highly smoothed version of the real situation. As mentioned above, the total energy dissipated is given by the area under $\tau(D)$, but it is not obvious how this energy is partitioned to thermal energy, fracture energy, and other forms of energies (e.g., latent heat if phase transitions of the material due to heating near the crack surface is involved) [Tinti et al., 2005]. In seismological applications, in order to circumvent this difficulty, the behavior is simplified as shown in Figure 2a. In this case, the stress drops from τ_P to a constant value τ_2 after slip D_c, and then stays at this constant level until the end of slip motion. This particular model is generally called the slip-weakening model [see Ida, 1972; Palmer and Rice, 1973, Li, 1987]. (Exactly what "slip-weakening" means is somewhat ambiguous.) By assuming this behavior, the dissipated energy can be partitioned to the fracture energy E_G and frictional energy E_F as shown in Figure 2a.

To understand this particular energy partition, it is convenient to consider an ideal case, as a reference model, given by the following thought process. Consider a crack on which the shear stress is reduced from τ_1 to τ_2. If the crack can extend without any resistance at the crack tip or any energy dissipation other than that due to surface friction, the stress can drop instantly from τ_1 to τ_2 and slip develops at τ_2. In this case, the dissipated energy is given by the rectangular area CBDO shown in Figure 2b, and this energy, given by $\tau_2 DA$, can be simply interpreted as interface frictional energy E_F which is often equated to the energy dissipated as heat, E_H. From Figure 2, the difference between the potential energy and E_F is equal to

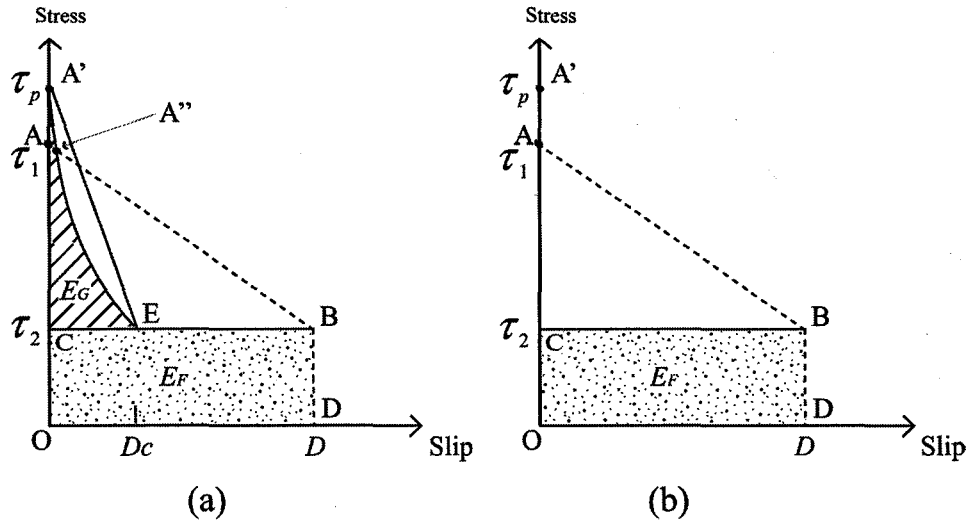

Figure 2. The variation of stress at a point on a fault as a function of slip. (a). A simplified model which is commonly referred to as "Slip-weakening model". (b). The ideal model without energy dissipation other than that due to friction on the fault plane.

$$E_{T0} = \frac{1}{2}(\tau_1 - \tau_2)DA \tag{4}$$

and this energy is available for rupture propagation. In this sense, E_{T0} is also called the available energy. The general slip-weakening case shown in Figure 2a is the case in which the extra amount of energy given by the hachured area A'A"EC is spent compared with the reference case (Figure 2b). This energy dissipation can be due to a combination of many processes. In the breakdown-zone model [e.g., Li, 1987], this is interpreted as the energy dissipated in the breakdown zone beyond the crack tip due to anelastic processes which may involve plastic yielding and micro cracking etc. All the energies associated with the different dissipative mechanisms are lumped together and the total is equated to E_G given by the hachured area. The rectangular area CBDO shown in Figure 2a is interpreted as the interface frictional energy, E_F, as is done for the simple case (Figure 2b). This is a conventional practice, and E_G is usually called the fracture energy in seismology, but, in effect, it is a sum of all kinds of energies associated with faulting, other than that due to interface friction. Thus, E_G is different from the fracture energy normally used in mechanics. It depends on not only the material, but also the process of faulting itself [e.g., Abercrombie and Rice, 2005]. For example, if faulting involves extensive off-fault cracking [Rice et al., 2005; Andrews, 2005], the energy used to create off-fault cracks may be included in E_G. If fault slip motion involves fluid pressurization or melting [Rice, 2006; Wibberley and Shimamoto, 2005] due to heating, the thermal energy and latent heat involved in melting and fluid pressurization can be also included in E_G. In this sense, we may call E_G the rupture energy to distinguish it from the fracture energy commonly used. In many numerical studies, E_G is often approximated by the triangular area A'EC, and is given by $E_G \approx (\tau_p - \tau_1)D_C A/2$, but this is just a matter of convenience. In fact, Guatteri and Spudich [2000] demonstrated that it is usually difficult to determine τ_P and D_C separately, and E_G given by the hachured area is the basic quantity that controls the rupture propagation, especially the rupture speed.

THEORETICAL MODEL VS. REAL FAULTS

The theoretical model from which equation (1) is derived is conceptually simple. On the right-hand side, the second term is the fracture energy spent at the fault tip in the classical sense, and the last term is the work done on the fault plane. All the energy dissipation occurs on the fault plane. In contrast, real faults involve energy dissipation in a volume surrounding the fault through grain crushing, off-fault cracking etc [Shipton et al., 2006a; Cocco et al., 2006]. In theory, this situation can be accommodated in the theoretical model if we introduce multiple faults. The surface Σ in (1) does not have to be a single surface. However, unless we know all the details of the geometry of the surfaces and stresses on them such a model is not practically useful. Thus, in the practice discussed in this paper, we approximate a fault by a single surface Σ, and include any energy sink near Σ in the last term as the work done on the fault plane. Other off-fault processes cannot be treated rigorously, but we incorporate them through the use of the slip-weakening model. In the slip-weakening model, we divide the dissipated energy into two parts. The

first part is the frictional energy loss due to constant friction on the fault plane and we assume that this constant frictional stress does not affect the rupture dynamics. It simply changes the magnitude of the effective stress acting on the fault plane. The second part is the rupture energy that is directly related to the process of advancing fault rupture, and we include the energy losses due to all the processes other than the constant interface friction. These energies include those due to plastic yielding near the advancing fault tip, off-fault cracking, thermal energies involved in fluid pressurization and melting. Although exactly which energy should be included in E_G is model dependent, this practice provides a useful working model for studying the physics of earthquakes with a tractable seismological approach.

OVERSHOOT AND UNDERSHOOT

As we discussed earlier, the commonly used slip-weakening model has a simple stress-slip function (e.g., A'A''EB in Fig. 2a), but the stress change during actual faulting can be more complex. As the next level of complexity to the simple slip weakening model, here we consider two simple models, overshoot and undershoot models. These models are often used in seismology [Savage and Wood, 1971; Madariaga 1976; Beeler et al. 2003]. An overshoot occurs if the fault moves past the equilibrium point corresponding to the final stress (because of the inertia) and is locked there due to friction. If there is no friction, it will oscillate around the equilibrium point, and eventually stops at the equilibrium point. In Figure 3a, the line AFB shows the static equilibrium unloading curve. Suppose a slip which is occurring at a constant friction τ_{F0} does not stop when the slip reaches the static equilibrium point F, overshoots and stops at G. Then, as soon as the slip stops, the stress drops to the equilibrium stress τ_2 corresponding to B. In this case, the total energy dissipated is $\tau_{F0}D$, and the available energy E_{T0}' is given by the difference between the areas ACB and ECBG,

$$E_{T0}^{'} = E_{T0} - (\tau_{F0} - \tau_2)DA = E_{T0}\left(1 - \frac{2\Delta\tau_{OS}}{\Delta\tau}\right) \quad (5)$$

where E_{T0} is given by (4) and

$$\Delta\tau_{OS} = \tau_{F0} - \tau_2 \quad (6)$$

is the overshoot stress. Madariaga (1976) showed that for a circular fault with a rupture speed V_R=0.9β, the overshoot is 20 % (i.e., $\frac{\Delta\tau_{OS}}{\Delta\tau}$=0.2).

The other case is undershoot (Figure 3b). If the slip stops prematurely at G after having encountered some barrier, the stress at the end changes from τ_{F0} to τ_2. Then

$$E_{T0}^{'} = E_{T0} + (\tau_2 - \tau_{F0})DA = E_{T0}\left(1 + \frac{2\Delta\tau_{US}}{\Delta\tau}\right) \quad (5')$$

where $\Delta\tau_{US} = \tau_2 - \tau_{F0} > 0$ is the undershoot stress.

These models are two realizations of the general case shown in Figure 1 and are intuitively useful.

FRICTIONAL ENERGY

Because there is no simple seismological method to determine the absolute level of stress on the fault, we can say little about the frictional energy from seismological data alone.

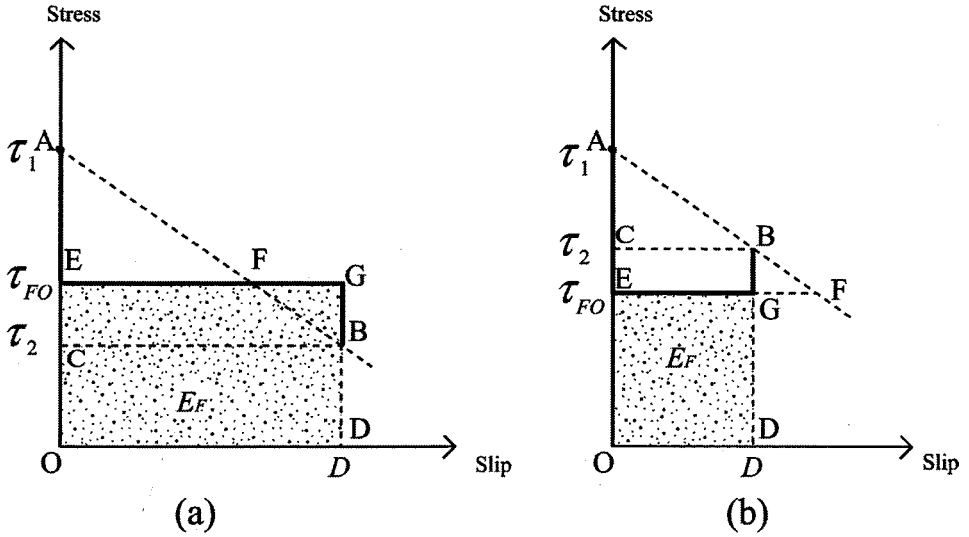

Figure 3. Overshoot (a) and undershoot (b) models.

Kanamori and Heaton [2000] argued that if a slip zone is narrow, 10 mm or less, as suggested by some field data [e.g., Sibson, 2003], the friction during fault motion is most likely very small for large earthquakes (M_w>7). If fluid exists in a fault zone and the permeability is sufficiently small, then fluid pressurization within the fault zone reduces the friction to essentially zero [Sibson, 1973; Mase and Smith, 1987; Andrews, 2002]. If no fluid exists, the friction can be initially high, but because of the localized slip zone, the temperature becomes high enough to cause melting, which will eventually lower the friction. It has been suggested that melting may initially increase friction thereby terminating slip motion. For large events, however, the slip is large so that it must have overcome this initial resistance, and the fault motion can occur at low friction. Thus, regardless of whether a fault zone is "wet" or "dry", the friction is most likely low for large events. However, if the coseismic slip zone is very wide, much larger than 10 cm, or faulting occurs on multiple strands simultaneously, fluid pressurization or melting may not occur, and friction can remain high.

Kano et al. [2006] made detailed temperature measurements in a borehole that intersects the Chelungpu fault which slipped about 4 m during the 1999 Chi-Chi Taiwan earthquake. They observed that the temperature anomaly that is attributed to frictional heating during coseismic slip was relatively small, and estimated that the coefficient of friction is about 0.08. Although the depth is only 1 km, this study demonstrates that a large coseismic slip did occur at very small friction.

Boullier et al. [2001] studied the properties of pseudotachylytes from the Nojima fault. Some parts of the Nojima fault ruptured in 1995 during the Kobe earthquake. They concluded that the pseudotachylytes were formed at a depth of at least 15 km, and melting must have occurred at a minimum temperature of 1200 °C. A very rapid acceleration and deceleration of fault motion is suggested. Since the thickness of pseudotachylytes is small, a modest level of friction is enough to raise the temperature necessary for melting. For example, if a fault zone is 1 cm thick, a frictional stress of 10 MP is enough to raise the fault zone temperature by 1000 °C for an M_w=7 earthquake [e.g., Kanamori and Heaton, 2000]. Thus, this study demonstrates that coseismic slip at the seismogenic depth (i.e., 15 km) can occur at low friction.

Since the field data are still limited, we cannot make a definitive conclusion about the level of friction, but the available field data and the simple argument on fluid pressurization and melting described above seem to indicate that relatively low frictional energy is involved in large earthquakes, but debates on this issue will undoubtedly continue.

ENERGY-MOMENT RATIO AND RADIATION EFFICIENCY

To relate the models described above to earthquake data, the simplest way is to use macroscopic parameters such as seismic moment M_0 and radiated energy E_R. These are the most commonly determined seismological parameters which can be estimated for most earthquakes, although estimations are difficult for small earthquakes because the radiated wave field is strongly influenced by small scale heterogeneities in the source and the propagation path, and the extensive energy attenuation and scattering along the wave path.

A simple parameter would be the ratio $\tilde{e} = E_R / M_0$. When multiplied by the rigidity μ, this quantity is called the apparent stress and has been used in seismology for a long time [Aki, 1966; Wyss and Brune, 1968; Wyss, 1970a, 1970b]. However, because of the large uncertainties in E_R, the significance of it was not obvious until recently when the accuracy of E_R determination has improved. Because it is called "stress", the apparent stress is frequently confused with other stresses. To avoid this confusion, here we use a non-dimensional parameter $\tilde{e} = E_R / M_0$ and call it the scaled energy. Since

$$\tilde{e} = E_R / M_0 = E_R / \mu DA = (1/\mu)(1/D)(E_R / A) \qquad (7)$$

(A=fault area, D=slip), $\tilde{e}$ is proportional to the radiated energy scaled by the fault area and slip. As such, it is a useful dynamic parameter of earthquakes, and has been used for purposes of comparing the dynamic characteristics of small and large earthquakes, and of earthquakes in different tectonic environments and depths.

Although $\tilde{e}$ can be estimated for many earthquakes, it cannot be readily related to the energy budget of an earthquake which, as we discussed above, provides a more useful link between macroscopic and microscopic physics of earthquakes.

A more useful parameter is the ratio of the radiated energy to the available energy E_{T0} (instead of M_0), $\eta_R = E_R / E_{T0}$, which can be written as

$$\eta_R = (2\mu / \Delta\tau)(E_R / M_0) = (2\mu\tilde{e} / \Delta\tau) \qquad (8)$$

η_R is called the radiation efficiency and has been used in the seismological literature for a long time [Husseini and Randall, 1976; Husseini, 1977]. However, because of the difficulty in estimating $\tilde{e}$ and $\Delta\tau$ accurately enough, η_R does not seem to have been used extensively until recently. With the availability of high-quality seismic data as well as the improvement of methods, it is becoming possible to characterize large earthquakes with this parameter [Venkataraman and Kanamori, 2004].

The radiation efficiency, η_R, is different from the seismic efficiency, η, which is given by the ratio of E_R to the total energy E_T, i.e. $\eta = E_R / E_T$. As mentioned earlier, because we cannot determine E_T, η cannot be estimated with seismological methods. In contrast, we can estimate η_R with the use of the slip-weakening model for studying the dynamic characteristics of earthquakes.

It should be noted that many assumptions, implicit or explicit, have been made in relating η_R to the physics of earthquake process. First, the basic "slip-weakening" model as illustrated in Figure 2 is assumed. As discussed earlier, the actual stress release pattern could be more complex than that shown in Figure 2. Second, overshoot and undershoot are not usually included in the analysis of seismic data, because no direct determinations of overshoot and undershoot have been made, though some efforts have been made to find observational evidence for and against them [e.g., Smith et al., 1991; Hwang et al., 2001]. If overshoot or undershoot is included, using (4) or (6), the radiation efficiency, η_R, can be written as

$$\eta_R = \eta_0' / (1 - 2\Delta\tau_{OS} / \Delta\tau) = \eta_0' / (1 + 2\Delta\tau_{US} / \Delta\tau) \quad (9)$$

where η_0' is the radiation efficiency estimated with the assumption of no overshoot or undershoot using equation 8; η_0' can be larger than 1. Third, Figure 1 is already a simplified model, and the actual stress release is a function of space and time given by equation (1). To use equation 1, we need to determine the slip and stress as a function of time and space on the fault plane. Recent studies [Ide 2002; Favreau and Archuleta, 2003] suggest that it is possible to estimate the radiated energy with this method. The results are in general consistent with those estimated from teleseismic P and S waves using the standard method.

RUPTURE SPEED AND EFFICIENCY

A rigorous treatment of this subject is beyond the scope of this paper. For some idealized geometries, theoretical results are available. However, faulting in real earthquakes occurs in complex media with non-uniform properties (e.g., non planar surface, jogs, etc) and in complex crustal structures with non-uniform velocity structures. Thus, the theoretical models cannot be used directly. Here, we use a simple intuitive approach following Mott [1948] [see also, Lawn, 1993; Husseini and Randall, 1976, Kanamori and Brodsky, 2004] in an attempt to provide a means for interpreting observed results.

Referring to the simple reference model we introduced earlier (Figure 2), we assume that a crack is driven by the stress concentration near the crack tip. For shear faults, most energy propagates at the speed of shear wave β or Rayleigh-wave speed C_R. However, a small amount of energy can propagate at P-wave speed, α, in certain geometries. Thus, the limiting speed of fault ruptures is expected to be β or C_R in most cases, but it could reach α in certain geometries. If there is no resistance or no energy dissipation other than that due to interface friction such as the case for the ideal reference model (Figure 2), the fracture at the tip is expected to occur immediately after the arrival of the stress wave caused by slip. Thus, the rupture is expected to propagate at the limiting speed, C_L, i.e., $V_R / C_L = 1$. In this case, since no energy dissipation is involved (i.e., $E_G = 0$), the radiation efficiency $\eta_R = 1$. In contrast, if some energy is required to advance the rupture front, the rupture is expected to slow down. In the extreme case of quasi-static rupture growth, no energy is radiated, i.e., $\eta_R = 0$, and $V_R \to 0$. Thus, η_R varies from 1 to 0, as V_R varies from C_L (=β in most cases) to 0. Various theoretical relations have been obtained as

$$\eta_R = 1 - g(V_R) \quad (10)$$

where

$$g(V_R) = 1 - V_R / C_R,\ g(V_R) = (1 - V_R / C_R) / \sqrt{1 - V_R / \beta},$$
$$\text{and } g(V_R) = \sqrt{\frac{1 - (V_R / \beta)}{1 + (V_R / \beta)}} \quad (11)$$

for Mode I (opening) cracks [Freund, 1972], Mode II (sliding) cracks [Fossum and Freund, 1975], and Mode III (tearing) cracks [Kostrov 1966; Eshelby 1969], respectively. A simple energy-based consideration leads to

$$g(V_R) = 1 - \frac{V_R^2}{C_L^2} \quad (12)$$

[Mott, 1948; Lawn, 1993; Kanamori and Brodsky, 2004]. These relations are sketched in Figure 4 as a function of V_R / β.

FAULT-ZONE STRUCTURE AND SEISMOLOGICAL PARAMETERS

A zone of crushed rocks, called fault gouge, is observed along faults. The width of the gouge layer, T, has been measured by various investigators [Robertson, 1982; Otsuki, 1978]. We can estimate the total fracture energy used to form the gouge layer as follows [Kanamori, 2004].

Suppose we consider an initially unbroken block of crustal rock. Then, after a fault has slipped many times, a gouge layer with a thickness T is formed. Let L be the fault length,

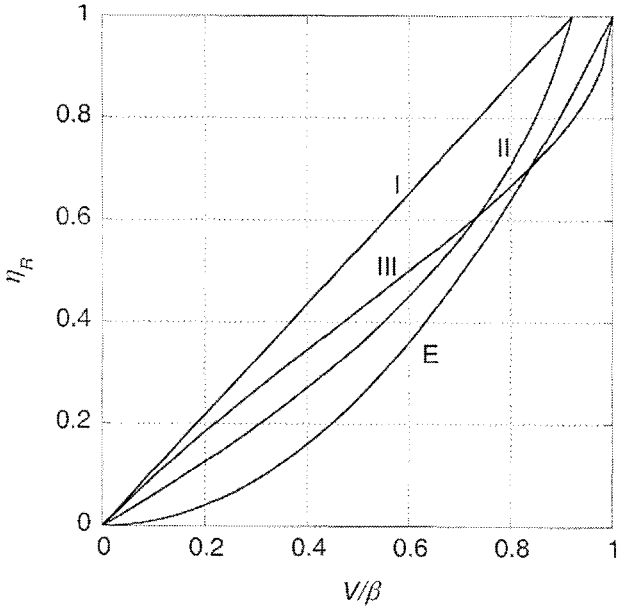

Figure 4. The radiation efficiency as a function of scaled rupture speed for four rupture models. Labels I, II, III, and E denote the relations for Mode I, Mode II, Mode III, and that given by (12), respectively.

and H be the width of the fault. Then $V=LHT$ is the volume of the gouge layer. Suppose that the gouge layer consists of grains with a representative radius a. The number of grains in this volume is $N = THL/(4\pi a^3/3)$ and the total surface area of the grains is $S_G = 4\pi a^2/N = 3TLH/a = 3TS/a$, where $S=LH$ is the fault area. If the fracture energy required to produce a new surface is G_c (per unit area), then the total fracture energy associated with the formation of the gouge layer is given by,

$$E_G = (G_c/2)\lambda S_G = 3\lambda G_c ST/2a = 3\lambda G_c M_0 (T/D)/(2\mu a) \quad (13)$$

where λ is a factor to correct for the difference between the geometrical and actual shapes of the grain. Here we use λ =6.6 (Wilson et al., 2005). Then the radiation efficiency η_R can be expressed as the ratio of the radiated energy E_R to the sum of E_R and the fracture energy E_G given above. Introducing an empirical relation $E_R = C_r M_0$ where C_r is an empirical constant, we obtain,

$$\eta_R = \frac{1}{1+\frac{3\lambda}{\mu C_r}\left(\frac{T}{D}\right)\left(\frac{G_c}{2a}\right)} \quad (14)$$

The specific fracture energy, G_c, for minerals and rocks ranges from 0.1 to 10 J/m^2 (Friedman et al., 1972; Scholz, 2002; Lawn, 1993) and here G_c =1 J/m^2 is used as a representative value, and C_r=5x10^{-5} is used as a representative value

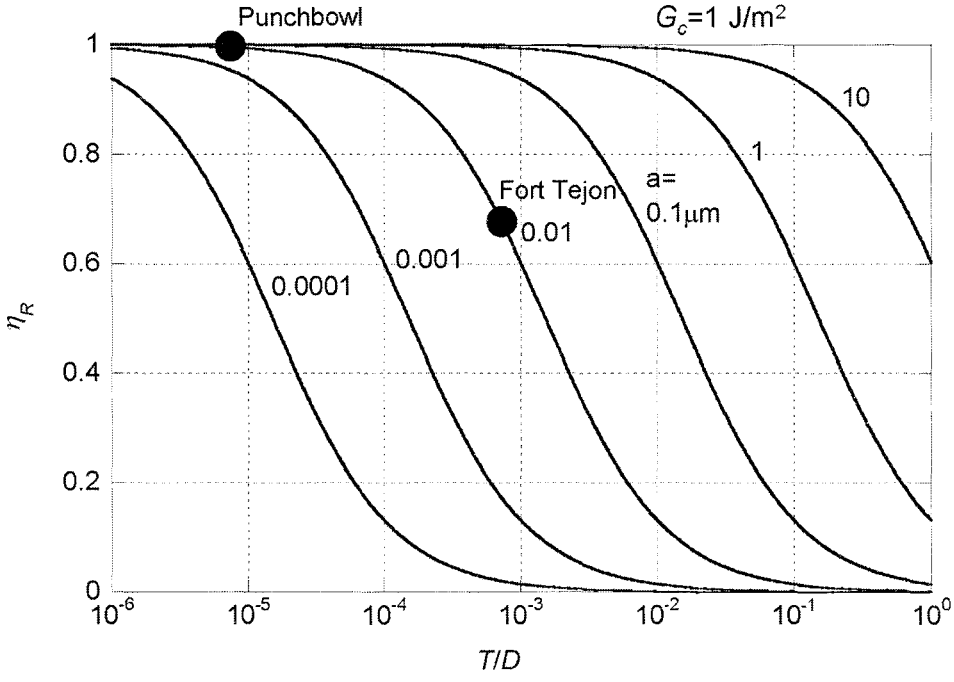

Figure 5. The relationship between the radiation efficiency, η_R, and the gouge thickness divided by the total displacement, T/D, with the grain size of the gouge as a parameter. The specific fracture energy for the fault gouge material, G_C, is assumed to be 1 J/m^2.

for strike slip earthquakes. Relation 14 is shown in Figure 5 with the grain size a as a parameter.

Wilson et al. [2005] and Chester et al. [2005] use $a \approx 10$ nm (0.01 μm). The results for the San Andreas fault near Fort Tejon [Wilson et al. 2005] and the Punchbowl fault in California [Chester et al., 2005] are plotted in Figure 5. These results show that the radiation efficiency, η_R, is approximately 0.7 and 1 for the San Andreas fault and the Punch Bowl fault respectively. For comparison, Venkataraman and Kanamori [2004] showed from seismological data that $\eta_R \geq 0.25$ for most shallow earthquakes.

We note here that many parameters (e.g., G_c, and C_r) and assumptions (e.g., uniform grain size) are used in this comparison, and interpretation of field data involves subjective judgments, especially on the definition of fault gouge. For example, Shipton et al. [2006b] divides fault zones to at least three components: principal slip surfaces, fault core, and damage zone. They are geometrically and mechanically distinct, and it is important to know exactly how fault rocks have been fractured. Also, at least three corrections must be made to E_G given by (13) before we can use it as the rupture energy in (14). First, if the interface friction is responsible for gouge formation the work done by friction must be subtracted from (13). Second, (13) does not include energies which were not used for crushing fault-zone rocks. Third, if healing of fault gouge has occurred, then E_G given by (13) is a lower bound. Despite all the uncertainties, we believe that the method described here with Figure 5 provides a useful tool for comparing field and seismological results through the radiation efficiency, η_R, for a wide range of assumptions.

CONCLUSION

In this short tutorial paper, we tried to relate the energies involved in earthquakes measured by seismological, geological, and other methods. In most seismological practices, the measured quantities are macroscopic in that they represent the energies involved in the whole process. The energy budget can be simply written as

$$E_T = E_R + E_{NR} \tag{15}$$

where E_T, E_R, and E_{NR} are the total potential energy change, the radiated energy, and the non-radiated energy, respectively. The radiated energy E_R can be estimated either from the energy flux at far field, or the displacement and stress change on the fault plane. Although accurate measurements are not always possible, its meaning is clear. However, we cannot measure E_T or E_{NR}, and without making further assumptions we cannot proceed beyond this point. In the procedure we discussed in this paper we divide E_{NR} into two terms:

$$E_{NR} = E_F + E_G \tag{16}$$

where E_F is the work done against the resistance to sliding on the fault plane and is called the frictional energy. With this division, we can write E_F as $E_F = \tau_2 DA$. E_G is the work done against the resistance to fault extension at the fault tip. We include in E_G all the energies due to plastic yielding and cracking (both near fault tips and off-fault) and latent heat due to thermal pressurization and melting etc. If we do this, then using the expression $E_T = (\tau_1 + \tau_2)DA/2$, we can rewrite (15) and (16) as

$$E_{T0} = E_R + E_G \tag{17}$$

where

$$E_{T0} = (\tau_1 - \tau_2)DA/2 = \Delta\tau DA/2 = M_0(\Delta\tau/2\mu) \tag{18}$$

Now, since both E_{T0} (equation 18) and E_R can be determined from seismological data, we can estimate the rupture energy E_G from (17). The energies E_G, together with E_F, can be compared to energies estimated from various field studies on fault gouge, pseudotachylytes, heat flows, temperature variations etc.

In the above, we simplified the problem to make it tractable with seismological approach. For example: (1) We use simple averages for displacement and stress on the fault plane which can be highly variable; (2) We use a simple relation between stress and slip (e.g., slip-weakening relation, Fig. 2a), but this relationship can be highly variable on the fault plane. (3) The distinction between the energy loss due to sliding friction on the fault plane and to other processes related to fault extension is not straightforward in general, and is model dependent. Exactly how valid these simplifications are is still vigorously debated.

One of the most challenging issues in these practices is how to average the highly variable slip, stress and frictional parameters to seismologically determinable macroscopic parameters.

To make further advances in this field the following are most important, many of which are already in progress.

1. Improvement of the accuracy of estimation of radiated energy. Introduction of three-dimensional structures and more detailed attenuation models is necessary.
2. Detailed mapping of slip and stress distributions on a fault plane to establish better averaging schemes for energy estimations.
3. Study of non-mechanical (e.g., thermodynamic) processes such as fluid pressurization and melting to assess their contributions to seismic energy budget.

4. Study of properties of fault gouge to understand their formation, deformation, and healing mechanisms.
5. Determination of the thickness of coseismic slip zone which is a key parameter for estimating the temperature and friction during faulting.
6. Mapping of complexity of fault geometry etc for understanding the spatial distribution of energy dissipation during coseismic slip.
7. Study of the properties of pseudotachylytes for understanding the temporal evolution of coseismic fault slip.
8. Study of frictional properties of solids under coseismic conditions (e.g., at high sliding speeds, at high confining pressures etc.).
9. Study of rupture processes under controlled environments in laboratory for understanding the effects of fault geometry and fault-zone structures on rupture speed and rupture direction.
10. Study of energy dissipation mechanisms in fluid-saturated materials to understand the energy budget of slow and silent earthquakes.
11. Study of the variability of earthquakes in terms of energy budget. (e.g., small vs. large, mature vs. immature faults, crustal (dip slip, strike slip) vs. subduction-zone earthquakes, shallow vs. deep earthquakes, slow vs. regular earthquakes).

Acknowledgments. This paper was based on the vigorous discussions at the Chapman Conference, and we thank all the participants for motivating us to write this paper. We thank Zoe Shipton, William Walter, and Rachel Abercrombie for a thoughtful review of the manuscript.

REFERENCES

Andrews, D. J. (2002), A fault constitutive relation accounting for thermal pressurization of pore fluid, *J. Geophy. Res., 107*, doi:10.1029/2002JB001942.

Andrews, D. J. (2005), Rupture dynamics with energy loss outside the slip zone, *Journal of Geophysical Research-Solid Earth, 110*, B01307, doi:01310.01029/02004JB003191.

Barenblatt, G. I. (1959), The formation of equilibrium cracks during brittle fracture: General ideas and hypothesis: Axially symetric cracks. Applied, *Mathematics ans Mechanics (PMM), 23*, 622–636.

Beeler, N. M., T. F. Wong, and S. H. Hickman (2003), On the expected relationships among apparent stress, static stress drop, effective shear fracture energy, and efficiency, *Bulletin of the Seismological Society of America, 93*, 1381–1389.

Boatwright, J., and G. Choy (1986), Teleseismic estimates of the energy radiated by shallow earthquakes, *J. Geophys. Res., 91*, 2095–2112.

Boullier, A.-M., T. Ohtani, K. Fujimoto, H. Ito, and M. Dubois (2001), Fluid inclusions in pseudotachylytes from the Nojima fault, Japan, *J. Geophys. Res., 106*, 21,965–21977.

Chester, J. S., F. M. Chester, and A. K. Kronenberg (2005), Fracture surface energy of the Punchbowl fault, San Andreas system, *Nature, 437*, 133–136.

Cocco, M., P. Spudich, and E. Tinti (2006), On the mechanical work absorbed on faults during earthquake ruptures, this issue.

Dahlen, F. A. (1977), The balance of energy in earthquake faulting, *Geophys. J. Roy. Astron Soc., 48*, 239–261.

Eshelby, J. D. (1969), The elastic field of a crack extending non-uniformly under general anti-plane loading, *J. Mech. Phys. Solids, 17*, 177–199.

Favreau, P., and R. J. Archuleta (2003), Direct seismic energy modeling and application to the 1979 Imperial Valley earthquake, *Geophysical Research Letters, 30 (5)*, 1198, doi:1110.1029/2002GL015968.

Fossum, A. F., and L. B. Freund (1975), Nonuniformly Moving Shear Crack Model of a Shallow Focus Earthquake Mechanism, *J. Geophys. Res., 80*, 3343–3347.

Freund, L. B. (1972), Energy flux into the tip of an extending crack in an elastic solid, *J. Elasticity, 2*, 341–349.

Friedman, M., G. Alani, and J. Handin (1972), Fracture-Surface Energy of Rocks, *International Journal of Rock Mechanics and Mining Sciences, 9*, 757–766.

Griffith, A. A. (1920), The phenomena of rupture and flow in solids, *Phil. Trans. Roy. Soc. of London, A 221*, 169–198.

Guatteri, M., and P. Spudich (2000), What Can Strong-Motion Data Tell Us about Slip-Weakening Fault-Friction Laws?, *Bull. Seismol. Soc. Am., 90*, 98–116.

Haskell, N. A. (1964), Total energy and energy spectral density of elastic wave radiation from propagating faults, *Bull. Seism. Soc. Am., 54*, 1811–1841.

Husseini, M. I. (1977), Energy balance for formation along a fault, *Geophys. J. Roy. Astron. Soc., 49*, 699–714.

Husseini, M. I., and M. Randall (1976), Rupture velocity and radiation efficiency, *Bull. Seismol. Soc. Am., 66*, 1173–1187.

Hwang, R. D., J. H. Wang, B. S. Wang, K. C. Chen, W. G. Huang, T. M. Chang, C. H. C., and C. C. Peter (2001), Estimates of stress drop of the Chi-Chi, Taiwan, earthquake of 20 September 1999 from near-field seismograms, *Bull. Seismol. Soc. Am., 91*, 1158–1166.

Ida, Y. (1972), Cohesive Force across Tip of a Longitudinal-Shear Crack and Griffiths Specific Surface-Energy, *Journal of Geophysical Research, 77*, 3796–3805.

Ide, S. (2002), Estimation of Radiated Energy of Finite-Source Earthquake Models, *Bull. Seism. Soc. Am., 92*, 2994–3005.

Ide, S., and M. Takeo (1997), Determination of constitutive relations of fault slip based on seismic wave analysis, *J. Geophys. Res., 102*, 27,379–327,391.

Jeffreys, H. (1942), On the mechanics of faulting, *Geol. Mag., 79*, 291–295.

Kanamori, H. (2004), The diversity of the physics of earthquakes, *Proceedings of the Japan Academy Series B-Physical and Biological Sciences, 80*, 297–316.

Kanamori, H., and E. E. Brodsky (2004), The physics of earthquakes, *Reports on Progress in Physics, 67*, 1429–1496.

Kanamori, H., and T. H. Heaton (2000), Microscopic and Macroscopic Physics of Earthquakes, in *Geocomplexity and the Physics of Earthquakes*, edited by J. B. Rundle, et al., pp. 147–163, AGU, Washington, DC.

Kano, Y., J. Mori, R. Fujio, H. Ito, T. Yanagidani, S. Nakao, and K.-F. Ma (2006), Heat signature on the Chelungpu fault associated with the 1999 Chi-Chi, Taiwan earthquake, *Geophy. Res. Lett., 33*, L14306, doi:14310.11029/12006GL026733.

Kostrov, B. V. (1966), Unsteady propagation of longitudinal shear cracks, *J. Appl. Math. Mech. (transl. P. M. M.), 30*, 1241–1248.

Kostrov, B. V. (1974), Seismic moment and energy of earthquakes, and seismic flow of rock (translated to English), *Izv. Earth Physics, 1*, 23–40.

Lawn, B. (1993), *Fracture of Brittle Solids—Second Edition*, 378 pp., Cambridge University Press, Cambridge.

Li, V. C. (1987), Mechanics of shear rupture applied to earthquake zones, in *Fracture Mechanics of Rock*, edited, pp. 351–428, Acdemic Press, London.

Madariaga, R. (1976), Dynamics of an expanding circular fault, *Bull. Seism. Soc. Am.*, *66*, 639–667.

Madariaga, R., J. P. Ampuero, and M. Adda-Bedia (2006), Seismic radiation from simple models of earthquakes, *this issue.*

Mase, C. W., and L. Smith (1987), Effects of frictional heating on the thermal, hydrologic and mechanical response of a fault, *J. Geophys. Res.*, *92*, 6249–6272.

McGarr, A., S. M. Spottiswoode, N. C. Gay, and W. D. Ortlepp (1979), Observations relevant to seismic driving stress, stress drop, and efficiency, *Journal of Geophysical Research*, *84*, 2251–2261.

Mikumo, T., K. B. Olsen, E. Fukuyama, and Y. Yagi (2003), Stress–breakdown time and slip–weakening distance inferred from slip–velocity functions on earthquake faults, *Bulletin of the Seismological Society of America*, *93*, 264–282.

Mott, N. F. (1948), Brittle fracture in mild steel plates, *Engineering*, *165*, 16.

Otsuki, K. (1978), On the relationship between the width of shear zone and the displacement along fault, *J. Geolog. Soc. Japan*, *84*, 661–669.

Palmer, A. C., and J. R. Rice (1973), Growth of Slip Surfaces in Progressive Failure of over- Consolidated Clay, *Proceedings of the Royal Society of London Series a— Mathematical Physical and Engineering Sciences*, *332*, 527–548.

Rice, J. R. (2006), Heating and weakening of faults during earthquake slip, *J. Geophys. Res.*, *111*, B05311, doi:05310.01029/02005JB004006.

Rice, J. R., C. G. Sammis, and R. Parsons (2005), Off-fault secondary failure Induced by a dynamic slip pulse, *Bull. Seismol. Soc. Am.*, *95*, 109–134.

Rivera, L., and H. Kanamori (2005), Representations of the radiated energy in earthquakes, *Geophysical Journal International*, *162*, 148–155.

Robertson, E. C. (1982), Continuous formation of gouge and breccia during fault displacement. In Issues in Rock Mechanics, paper presented at Symp. Rock Mech. 23rd, Am. Inst. Min. Eng., New York.

Rudnicki, J. W., and L. B. Freund (1981), On energy radiation from seismic sources, *Bull. Seism. Soc. Am.*, *71*, 583–595.

Savage, J. C., and M. D. Wood (1971), The relation between apparent stress and stress drop, *Bull. Seismol. Soc. Am.*, *61*, 1381–1388.

Scholz, C. (2002), *The Mechanics of Earthquakes and Faulting, 2nd Ed.*, 496 pp., Cambridge Univ. Press, Cambridge.

Shipton, Z. K., J. P. Evans, R. Abercombie, and E. E. Brodsky (2006a), The missing sinks: Slip localization in faults, damage zones, and seismic energy budgets, *this issue.*

Shipton, Z. K., A. Soden, J. Kirkpatrick, and A. Bright (2006b), How thick is a fault? Fault displacement–thickness scaling revisited, *this issue.*

Sibson, R. H. (1973), Interactions between temperature and fluid pressure during earthquake faulting—A mechanism for partial or total stress relief, *Nature*, *243*, 66–68.

Sibson, R. H. (1975), Generation of pseudotachylyte by ancient seismic faulting, *Geophysical Journal of the Royal Astronomical Society*, *43*, 775–794.

Sibson, R. H. (2003), Thickness of the seismic slip zone, *Bull. Seismol. Soc. Am.*, *93*, 1169–1178.

Smith, K. D., J. N. Brune, and K. F. Priestley (1991), The seismic spectrum, radiated energy, and

Savage and Wood inequality for complex earthquakes, *Tectonophysics*, *188*, 303–320.

Terada, T. (1930), On the heat generated by the deformation of the Earth crust, *Bull. Earthq. Res. Inst. Tokyo Univ.*, *8*, 377–383.

Tinti, E., P. Spudich, and M. Cocco (2005), Earthquake fracture energy inferred from kinematic rupture models on extended faults, *J. Geophys. Res.*, *110*, B12303, doi:12310.11029/12005JB003644.

Venkataraman, A., and H. Kanamori (2004), Observational constraints on the fracture energy of subduction zone earthquakes, *J. Geophys. Res.*, *109*, B05302, doi:05310.01029/02003JB002549.

Wibberley, C. A. J., and T. Shimamoto (2005), Earthquake slip weakening and asperities explained by thermal pressurization, *Nature*, *436*, 689–692.

Wilson, B., T. Dewers, Z. Reches, and J. Brune (2005), Particle size and energetics of gouge from earthquake rupture zones, *Nature*, *434*, 749–752.

Wyss, M. (1970a), Stress estimates for south American shallow and deep earthquakes, *J. Geophys. Res.*, *75*, 1529–1544.

Wyss, M. (1970b), Apparent stress of earthquakes on ridges compares to apparent stresses of earthquakes in trenches, *Geophys. J. R. astr. Soc.*, *19*, 479–484.

Wyss, M., and J. N. Brune (1968), Seismic moment, stress, and source dimensions for earthquakes in the California–Nevada region, *J. Geophys. Res.*, *73*, 4681–4694.

Hiroo Kanamori, Seismological Laboratory, California Institute of Technology, Pasadena, California 91125

Luis Rivera, EOST–IPGS; Université Louis Pasteur, 5, Rue René Descartes, F67084, Strasbourg, France